$V_x(z)$ = longitudinal velocity as function of depth (m/s);
$\overline{V}_x$ = mean longitudinal flow velocity (m/s);
W_* = dimensionless settling velocity;
w_{ij} = settling velocity of grain size interval i of mineral density j (m/s);
x = distance along axis parallel to bed in flow direction (m);
x' = vertical profile correction factor in James entrainment function;
y = distance along axis parallel to bed in cross-flow direction (m);
z = distance normal to bed (m);
z_{bij} = bed elevation attributable to ith grain size fraction of mineral density j (m);
$\tan \alpha$ = dynamic friction coefficient in modified Bagnold equation;
β = bed slope angle;
ε_s = sediment eddy diffusion coefficient in vertical (m^2/s);
ε_z = fluid eddy diffusion coefficient in vertical (m^2/s);
Θ_{c50} = dimensionless critical shear stress necessary to entrain median grain diameter;
Θ_0 = dimensionless bed shear stress;
Θ_{cij} = dimensionless critical shear stress necessary to entrain grain i of mineral density j;
κ = von Karman's constant;
ν = kinematic fluid viscosity;
ρ = fluid density (kg/m^3);
σ_j = mineral density j (kg/m^3);
σ_τ = standard deviation of shear stress distribution (Pa);
τ' = instantaneous effective bed shear stress (Pa);
τ_{cij} = critical bed shear stress necessary to entrain grain size i of mineral density j (Pa);
τ_{c50} = critical bed shear stress necessary to entrain median grain diameter (Pa);
$\overline{\tau}'$ = skin friction component of time-averaged, median bed shear stress (Pa);
Φ = weighting factor for Preissman difference scheme; and
ϕ = grain pivot angle.

Subscripts and Superscripts

a = at height a above bed;
b = bedload;
i = grain size interval;
j = mineral density;
k = shear stress interval number;
nd = node number;
s = suspended load;
z = at height z above bed; and
$'$ = skin friction component.

Routing of Heterogeneous Sediments over Movable Bed: Model Verification

By Koen R. Vogel,[1] Andre van Niekerk,[2] Rudy L. Slingerland,[3] and John S. Bridge[4]

Abstract: A one-dimensional numerical model of heterogeneous size-density sediment transport has been developed to simulate the movement of graded sediments in natural and laboratory flow reaches. Predicted temporal and spatial variations in bed and armor-layer grain size distributions, eroded grain size distribution, eroded thicknesses, and total bedload transport rates compare quite favorably to observed variations in flumes, the San Luis canal, Colorado, and the East Fork River, Wyoming, for a large variety of flow scales and flow conditions. The main advantages of this model over others is the high degree of accuracy of model results obtained using only bed and flow variables as input, the treatment of turbulent fluctuations of bed shear stress, the minimization of calibration factors, and the explicit treatment of multiple grain densities. In addition, only the active layer thickness must be calibrated.

Introduction

A model investigating density and size sorting (MIDAS) has been developed (van Niekerk et al. 1992) to predict the transport of heterogeneous size-density sediments under nonuniform, quasi-unsteady, cross-sectionally averaged flow conditions. MIDAS was developed to accurately predict temporal and spatial variations in: (1) The flow field; (2) the size-density distributions of the bed material; (3) total transport rates of all size-density fractions making up the bed; and (4) bed degradation and aggradation.

The purpose of this article is to demonstrate that MIDAS performs well when compared against flume data of Little and Mayer (1972) and Ashida and Michiue (1971), and field data from the San Luis Valley canals collected by Lane and Carlson (1953) and from the East Fork River data collected by Leopold and Emmett (1976) and Mahoney et al. (1976). In addition, its use in predicting the occurrence of heavy mineral placers in a generic alluvial fan is demonstrated.

Specific Formulation of Model

The input parameters used in the model (van Niekerk et al. 1992) can be divided into three categories: (1) Physical constants known with some precision, e.g., the gravitational acceleration, dynamic viscosity of fluid, etc.; (2) numerical parameters used in discretization and solution schemes, e.g., the number of distance steps or the number of shear stress intervals; and (3) parameters defining how the model approaches the physics of the prob-

[1]Grad. Student, Dept. of Geosciences, Pennsylvania State Univ., University Park, PA 16802.
[2]Grad. Student, COMRO, P.O. Box 91230, Auckland Park, 2006 Republic of South Africa.
[3]Prof., Dept. of Geosciences, Pennsylvania State Univ., University Park, PA.
[4]Prof., Dept. of Geological Sciences, SUNY-Binghamton, Binghamton, NY 13901.

Note. Discussion open until July 1, 1992. Separate discussions should be submitted for the individual papers in this symposium. To extend the closing date one month, a written request must be filed with the ASCE Manager of Journals. The manuscript for this paper was submitted for review and possible publication on March 15, 1991. This paper is part of the ***Journal of Hydraulic Engineering,*** Vol. 118, No. 2, February, 1992. ©ASCE, ISSN 0733-9429/92/0002-0263/$1.00 + $.15 per page. Paper No. 1552.

lem, e.g., which physical laws and constants to use. Because the latter values are the least well constrained, some attention to them is warranted. In all runs presented here, turbulence was simulated by a Gaussian-distributed bed shear stress, with a coefficient of variation of 0.4, while the thickness of the moving bed layer was determined using the Einstein equation (van Niekerk et al. 1992)

$$a = 2D_{50} \quad \ldots\ldots (1)$$

in which a = the grain saltation height; and D_{50} = the median grain diameter. Grain mobility was modeled using a Komar (1989) entrainment function

$$\frac{\Theta_{cij}}{\Theta_{c50}} = \left(\frac{D_{ij}}{D_{50}}\right)^{-0.65} \quad \ldots\ldots (2)$$

in which Θ_{cij} = the critical Shields parameter for the ith size and jth density fraction; Θ_{c50} = the critical Shields parameter for the median grain diameter; D_{ij} = the grain diameter of grain size-density fraction ij; and D_{50} = the median grain size of the active layer. The active layer thickness was determined at the start of each numerical experiment as

$$T_a = 2D_{50}\frac{\bar{\tau}'}{\tau_{c50}} \quad \ldots\ldots (3)$$

in which T_a = the active layer thickness; $\bar{\tau}'$ = the effective temporal mean bed shear stress; and τ_{c50} = the critical shear stress necessary to entrain the median grain diameter. Active layer thickness was not allowed to vary dynamically during the experiments presented here, because at high flow strengths [e.g., Ashida and Michiue (1971), run 6], a dynamic thickness made MIDAS numerically unstable. However, at lower flow strengths, such as in most of the runs presented here, a dynamic active layer thickness presented no problems and, in fact, led to improved results. In the following discussion, it should be kept in mind that all the input parameters have either fixed values or values variable in a narrow range. In every case, the actual flow and grain size values were used as input. No parameter was adjusted in order to obtain a better fit.

In a series of sensitivity experiments performed on data from Little and Mayer's (1972) runs 1-2, 3-4, and 4-1, the thickness of the active layer was varied. Eq. (3) represents the best-fit equation for the active layer thickness, assuming that the active layer is a function of D_{50}, $\bar{\tau}'$, and τ_{c50}. Eq. (3) was then used to determine active layer thicknesses for the Ashida and Michiue, San Luis Valley canal, and East Fork River studies.

Sensitivity experiments also indicate the model matches Little and Mayer's and Ashida and Michiue's data, as well as the East Fork River data, as long as the distance step and the time step are chosen sufficiently small such that the transported sediment does not travel farther than one distance step over a single time step. While this rule provides a conservative estimate of the time step and distance step, larger time and distance steps can be chosen, providing the flow is fairly steady.

Flume Study of Little and Mayer (1972)

Little and Mayer (1972) investigated the effects of sediment gradation on channel armoring. A nonuniform sand-gravel bed was placed in a flume

measuring 12.2 m long, 0.6 m wide, and 0.1 m high. Clear water was passed over the bed to produce bed degradation and armoring. The eroded sediment was caught by screen separators at the downstream end of the flume, and at regular intervals was dried, weighed, and stored for later sieving. When the total transport rate was 1% of the original transport rate and the armoring was thought complete, the flume was drained and the armor layer was sampled using a molten beeswax method described by the authors (Little and Mayer 1972). MIDAS is tested against their run 3-4 (Table 1). The grain size distribution of the bed material (Table 2) is taken from Little and Mayer's Table 3, and normalized so that the cumulative weight percentage equals 100%.

For modeling purposes, the flume was divided into eight sections, each of 1.525 m length. The time step was 1 min. The active layer thickness, calculated from (3), was set to 0.002 m. The bed shear stress was not partitioned into form and skin components because bed forms were not present.

The measured and computed total transport rates (Fig. 1) show good

TABLE 1. Flow Variables Used in Computer Simulations

Data source (1)	Water discharge (m^3/s) (2)	Energy slope (3)	Manning's n ($m^{1/6}$) (4)	Water depth (m) (5)
Little and Mayer				
Run 3-4	0.016	0.0019	0.0153	0.066
Ashida and Michiue				
Run 2	0.03	0.0044	0.017	0.065
Run 6	0.0314	0.01	0.02	0.06
Lane and Carlson				
Test Section 12	2.8	0.0024	0.024	0.49
Gold Placer Study	100.0	0.00001	0.04	4.75

TABLE 2. Grain Size Distributions of Parent Bed Material

Little and Mayer		Ashida and Michiue		Lane and Carlson	
Grain size interval (mm) (1)	Weight (%) (2)	Grain size interval (mm) (3)	Weight (%) (4)	Grain size interval (mm) (5)	Weight (%) (6)
0.125–0.177	1.87	0.20–0.30	7.5	0.037–0.075	2.4
0.177–0.250	3.23	0.30–0.40	12.5	0.075–0.149	1.6
0.250–0.354	6.85	0.40–0.60	16.0	0.149–0.297	5.7
0.354–0.500	9.65	0.60–0.80	4.0	0.297–0.590	10.1
0.500–0.707	13.24	0.80–1.00	4.0	0.590–1.190	12.0
0.707–1.000	15.45	1.00–1.50	7.0	1.190–2.380	9.2
1.000–1.414	14.78	1.50–2.00	4.0	2.380–4.760	5.4
1.414–2.000	11.91	2.00–3.00	9.0	4.760–9.525	13.3
2.000–2.828	11.57	3.00–4.00	9.0	9.525–19.05	17.9
2.828–4.000	6.15	4.00–6.00	19.0	19.05–38.10	13.2
4.000–5.657	3.34	6.00–8.00	6.0	38.10–76.20	9.2
5.657–8.000	1.95	8.00–10.0	2.0	—	—

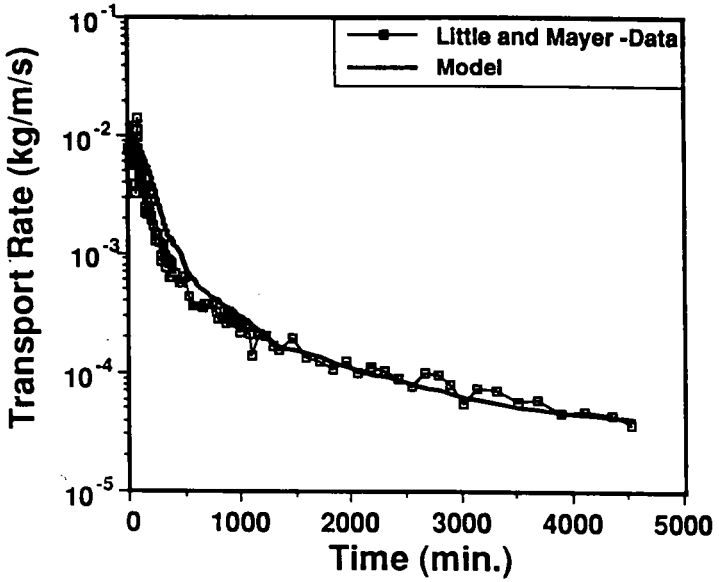

FIG. 1. Measured and Computed Sediment Transport Rate versus Time for Little and Mayer's Run 3-4

agreement, with the computed values within a factor of two of the measured values at all times. Local fluctuations in the measured transport rates, the origins of which are unknown, cause only temporary divergence of the two curves. It may be, as Little and Mayer (1972) claim, that the turbulence spectrum produces random and intermittent movement of the bed particles. The size distributions of the original sediment, the bed armor sediment, and the total eroded sediment (Fig. 2) after 75.5 hr of flow, show that the modeled armor layer is slightly finer than observed, although the difference in median grain sizes is only 0.3 mm (2.7 mm versus 3 mm). The reproduced and observed grain size distributions of the eroded sediment are practically coincident.

Flume Study of Ashida and Michiue (1971)

Ashida and Michiue (1971) investigated bed degradation and armoring by performing a series of flume experiments in which slope and discharge were varied. Both flow conditions and bed sediment material were selected to induce armoring. Clear water was allowed to flow over a 20-m long, 0.8-m wide flume filled with sediment of the grain size distribution given in Table 2. The weight percentages of the various grain size fractions were read from Ashida and Michiue's Fig. 1. Two runs, Ashida and Michiue's run 2 and run 6, were selected for comparison with MIDAS (Table 1).

For modeling purposes, the flume was divided into 20 equal intervals. The model time step was 1 min, and both runs were computed over the full 600 min of the flume study. Active layer thicknesses were 0.006 m for run 2 and 0.009 m for run 6, following (3). Water surface elevation at the most downstream node was kept constant to simulate the effects of the flume

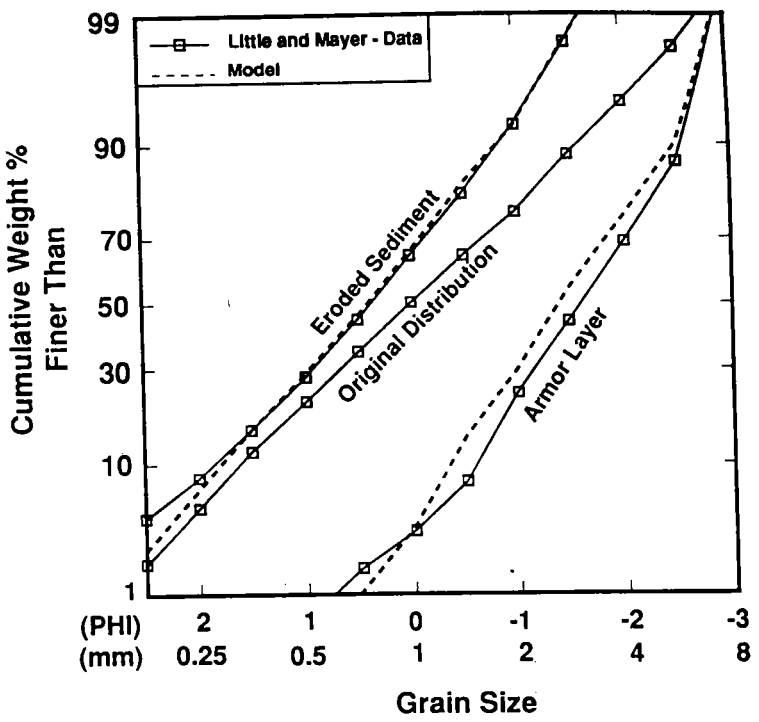

FIG. 2. Measured and Computed Grain Size Distributions for Little and Mayer's Run 3-4 after 75.5 hr of Flow

weir. Computed and measured grain size distributions of the armor layer and the eroded sediment (Fig. 3) compare well for run 2. The coarsest 70% of the armor grain size distributions are nearly coincident, and the median grain diameters are close (3.2 mm computed against 3.5 mm measured). The finest 30% of the computed armor layer diverges from the measured curve. Without more information on the sampling techniques used by Ashida and Michiue, it is difficult to comment on the origin of this discrepancy, although it may be due to inadvertent sampling of the subarmor layer. It should be noted that if the James or the Egiazaroff entrainment functions (van Niekerk et al. 1992) were substituted for (2), the finer sediment would be better protected against entrainment, because for low D_{ij}/D_{50}, the critical shear stress necessary to entrain a grain as predicted by these functions becomes infinite. The computed distribution of eroded sediment corresponds well with the measured curve, although the finer sediment tends to be overeroded in the model. The computed and measured median grain sizes of the eroded sediment are close (0.52 mm computed versus 0.61 mm measured).

Fig. 4(a–c) show the computed versus measured grain size distribution of the armor layer for run 6 at selected locations in the flume. While the trend towards a coarser bed layer is similar for the computed and measured curves for all three figures, the computed and measured median grain sizes

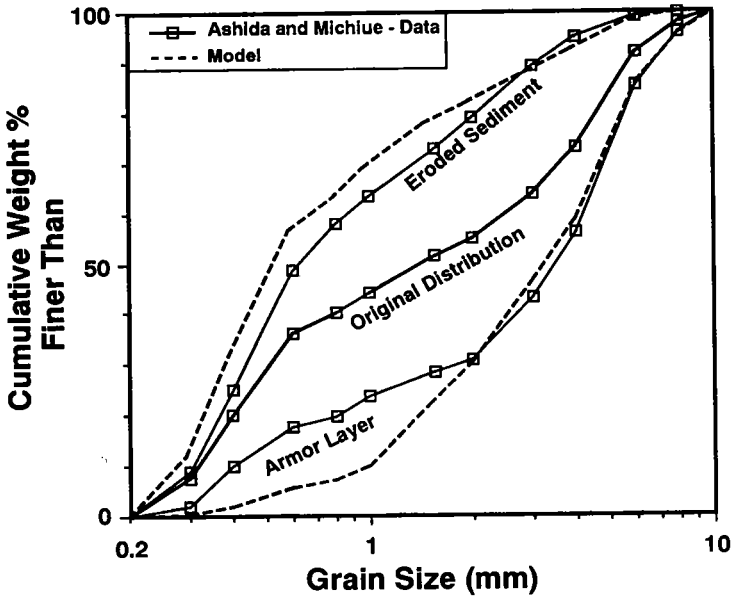

FIG. 3. Measured and Computed Grain Size Distributions for Ashida and Michiue's Run 2 after 600 min of Flow

differ significantly during the earlier run portions. The cause of this discrepancy is made apparent when the thickness eroded is plotted versus time (Fig. 5). Although the shape of the modeled curves agrees with the data, the amounts of erosion are underpredicted in the early stages of the run. This is possibly due to the nature of the flow. The Froude number during most of Ashida and Michiue's flume experiment was only slightly under unity. As most of the equations used in MIDAS (van Niekerk et al. 1992) were developed for natural stream applications, their accuracy at high Froude numbers is unclear. De Vries (1973) claims that uncoupled models, such as MIDAS, can only be used for flows with Froude numbers less than approximately 0.7. The underprediction could also be due to flume entrance effects, bedform effects in the flume, or due to the nonvariable active layer thickness used in the model. Eventually, as the modeled bed armors, the curves converge, and the total amounts eroded are well reproduced by the model. Thus, in the starting stages, the model underpredicts the removal of fines and total degradation of the bed, and consequently, the grain size distributions and thicknesses eroded do not match. Eventually the model converges to the correct equilibrium solution, and accurately reproduces the total eroded thickness and the grain size distribution at every location in the flume.

Field Study of Lane and Carlson (1953) (San Luis Valley)

In an attempt to perfect methods of stable canal design in coarse, noncohesive sediment, Lane and Carlson (1953) studied a number of stable canals constructed in the late 19th century in the San Luis Valley of south-

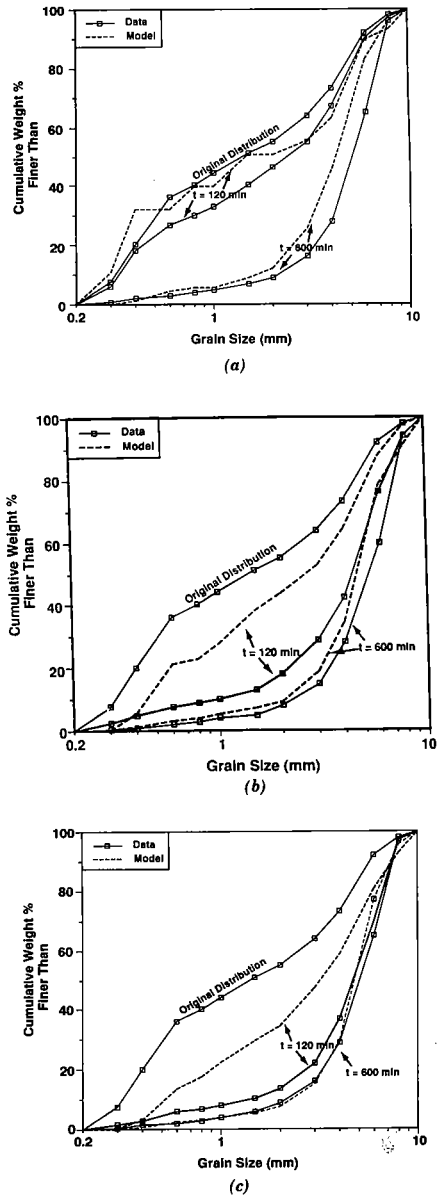

FIG. 4. Measured and Computed Grain Size Distributions for Ashida and Michiue's Run 6: (a) At 1 m Upstream from Weir; (b) At 10 m Upstream from Weir; (c) At 13 m Upstream from Weir

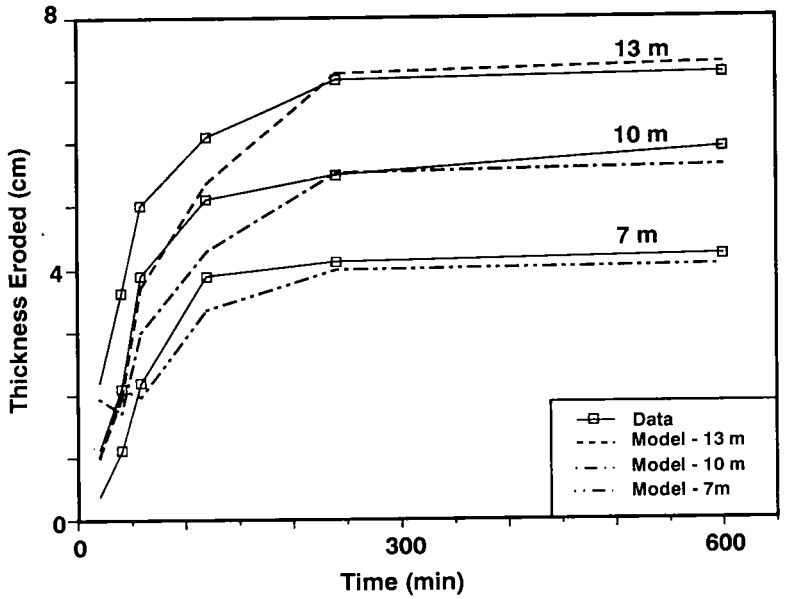

FIG. 5. Computed versus Measured Thicknesses Eroded at Various Locations Upstream from Weir for Ashida and Michiue's Run 6

central Colorado. They measured hydraulic parameters and bank and bed grain sizes at several test locations, thereby providing data on large-scale armoring over decades. Following Borah et al. (1982), test section 12, described by Lane and Carlson (1953), was selected. Because the armoring of the channel bed and walls must have occurred over the decades since the construction of the channels and much of the flow history over that period is unknown, the channel flow was modeled as follows. Flow variables, summarized in Table 1, were obtained from Lane and Carlson's 1950 measurements in their Table I. The lowest discharge mentioned by Lane and Carlson, 2.8 m^3s^{-1} (99 cfs), was selected as the model discharge, as it was felt that this was a more conservative estimate of the average channel flow than the maximum sustained discharge of 3.8 m^3s^{-1} (135 cfs) (Lane and Carlson 1953). This discharge was allowed to act on a 60-m long channel reach, divided into 5-m segments. The time step was 5 min. Partitioning of bed shear stress into skin and form friction was allowed and calculated using Einstein's reduction scheme (van Niekerk et al. 1992). The original size distribution of the bed material was taken to be the bank material obtained through canal wall excavation by Lane and Carlson (Table 2).

After 5 hr of model simulation, most of the material finer than 5 mm has been eroded out of the bed (Fig. 6). After 50 hr only the 19-, 38-, and 76-mm grain sizes remain in significant quantities. These correspond to the three sizes that make up 99% of the bed, as reported by Lane and Carlson. The computed percentages are different however, being 43% compared to a measured 9% for the 19-mm fraction, for example. This difference would decrease were the simulation run longer or run at the higher discharges, e.g., the "maximum sustained discharge," reported by Lane and Carlson

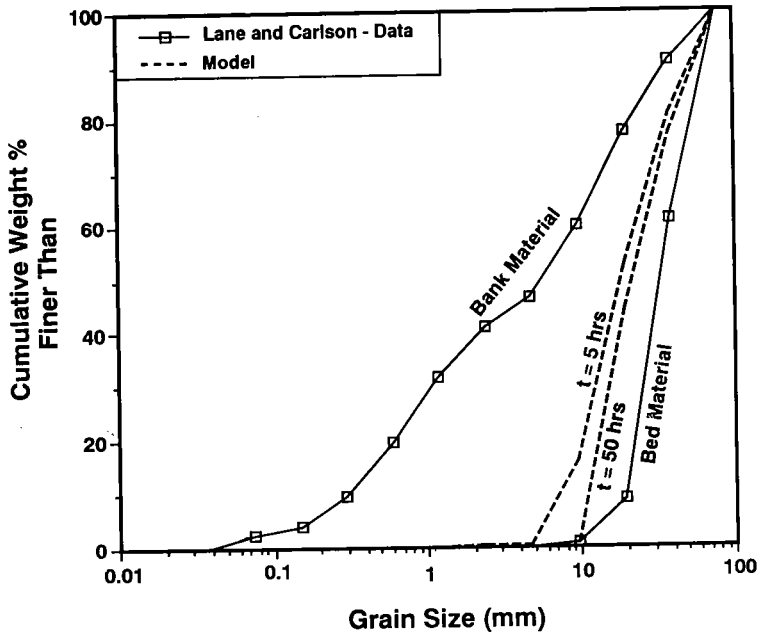

FIG. 6. Grain Size Distributions of Excavated Bank Material, of Present-Day Bed Material (Lane and Carlson 1953), and of Modeled Bed Grain Size Distribution at Various Time Stages for Lane and Carlson's Test Section 12

(3.6 m^3s^{-1} and 3.8 m^3s^{-1}). Because the complete flow history is unknown, this experiment was not done.

Field Study of Leopold and Emmett (1976) (East Fork River)

Sediment transport and hydraulic data were collected by the U.S. Geological Survey from a bedload trap and flow gages operated between 1973 and 1979, on the East Fork River, Wyoming (Leopold and Emmett 1976; Mahoney et al. 1976). A 5-km reach upstream from the bedload trap provides an ideal test of a model's ability to reproduce large-scale, nonuniform, unsteady flow and sediment transport. For modeling purposes, the reach was divided into 13 equally spaced intervals, such that the interval midpoints correspond roughly to stations B5 to B17 of Mahoney et al. (1976). At each node, a bed grain size distribution was synthesized from 20 size fractions ranging between 0.0625 and 45.3 mm diameter, based on an interval average of the measured bed grain size distributions. The simulated period extends from May 28, 1975, the day Leopold and Emmett measured the bed grain size distribution, to June 19, 1975. Two floods are contained in this period (Fig. 7). The water discharge and flow depth at the downstream node (B17), obtained from Leopold and Emmett's Table 1 (1976), were assumed to be constant for a 24-hr period corresponding to the measurement day. Rectangular cross sections were assumed, and widths at all nodes were kept constant in time. The bed shear stress was reduced using the algorithm described in van Niekerk et al. (1992), to simulate the effect of bedforms

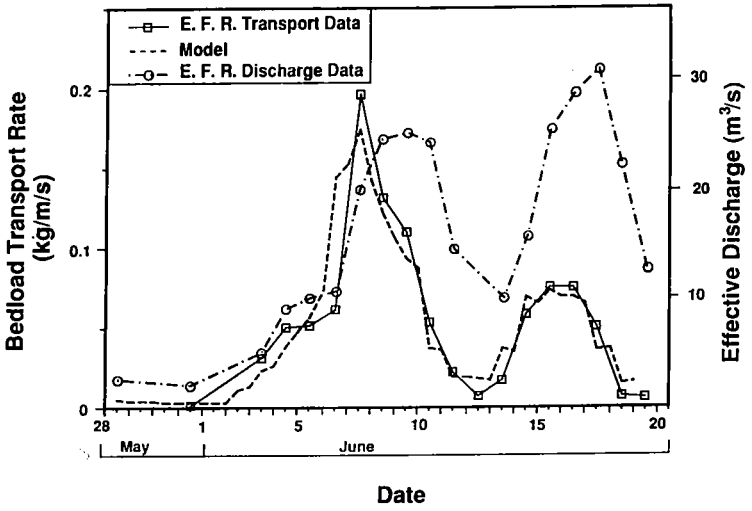

FIG. 7. Computed and Measured Bedload Transport Rates, and Measured Effective Discharge [as Defined by Leopold and Emmett (1976)] versus Time at USGS Facility, East Fork River, Wyoming, for Period of May 28–June 19, 1975

on the effective bed shear stress. Sediment influx at the upstream node (B5) was set equal to a value in equilibrium with the flow and the bed. Sediment influx from Muddy Creek, a tributary, was ignored because it consists primarily of fines. The time step was 10 min, and the active layer thickness, calculated from (3), was set to 0.005 m. The modeled bedload transport rates (dry weight transported through section B17 per second per meter width) compare favorably with the measured values obtained from Leopold and Emmett (1976) (Fig. 7). The width used as a denominator for the measured values is 14.8 m, the width of the bedload trap. The modeled bedload transport peaks match those recorded by Leopold and Emmett in both magnitude and date, for both flood events. More importantly, the model accurately reproduces the grain size distribution of the transported bedload (Fig. 8). On June 2, 1975, before the first flood, the median size of the bed was about 0.6 mm [Fig. 8(*a*)]. By June 7, 1975, at the height of the flood, both the measured and modeled grain size distributions had coarsened, such that the median was about 1.2 mm [Fig. 8(*b*)]. By June 11, 1975, after the flood wave had passed, measured and modeled grain size distributions of the bedload shifted back toward finer sizes, with medians of 1 and 1.4 mm, respectively [Fig. 8(*c*)]. This minor discrepancy may be due to the fact that the fine sediment influx from Muddy Creek was intentionally not modeled.

Curiously, the second flood, occurring between June 11 and 19, 1975, produced lower bedload transport rates than the first flood, although its peak water discharge was 19% higher (Fig. 7). The reason for this is obvious when the modeled median grain size of the bed material immediately upstream from the trap is compared for both flow events. At the start of the run (May 28), nodes B10 and B11 both had measured median grain sizes of 0.9 and 0.5 mm, respectively, values which were finer than the average of the reach. By June 3, just before the first flood event, this area of fine

sediment had migrated downstream to sections B13 and B14, just upstream from the bedload trap at B17. At the peak of the flood event (June 7), the readily entrainable fine sediment was transported to the bedload trap. By June 11, after the first flood, most sections were depleted in fine sediment, so that during the second flood, transport rates were lower. The first flood had partially armored the bed. Fig. 8(*d*), which compares the measured bedload grain size distributions during the peak of the two flood events confirms this interpretation, because during the second flood the bedload grain size distribution was measurably coarser.

Because the East Fork River study represents a fairly typical engineering

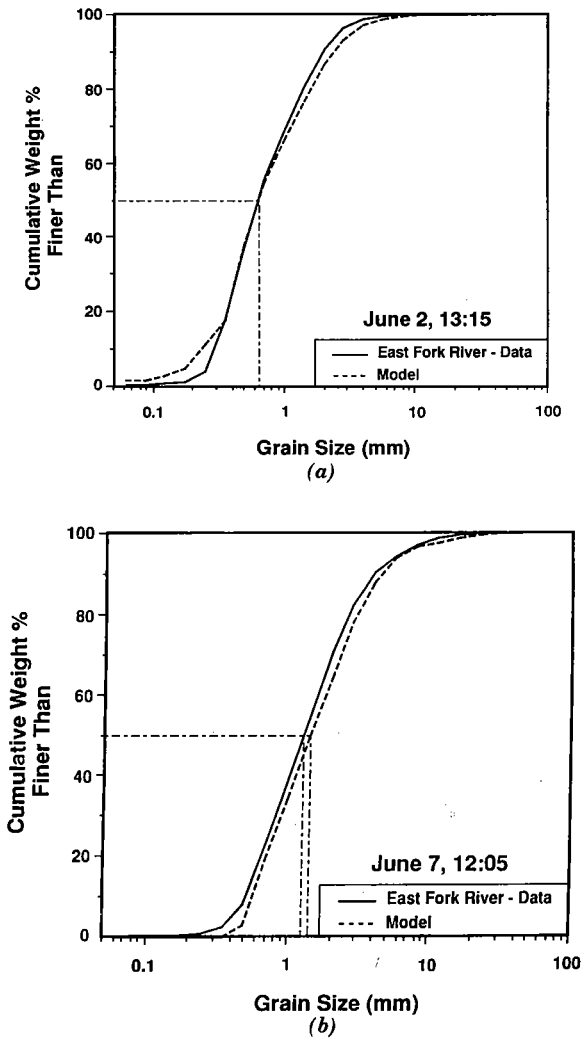

FIG. 8. Computed versus Measured Bedload Grain Size Distributions for East Fork River: (*a*) at 1:15 A.M. on June 2; (*b*) at 12:05 on June 7.

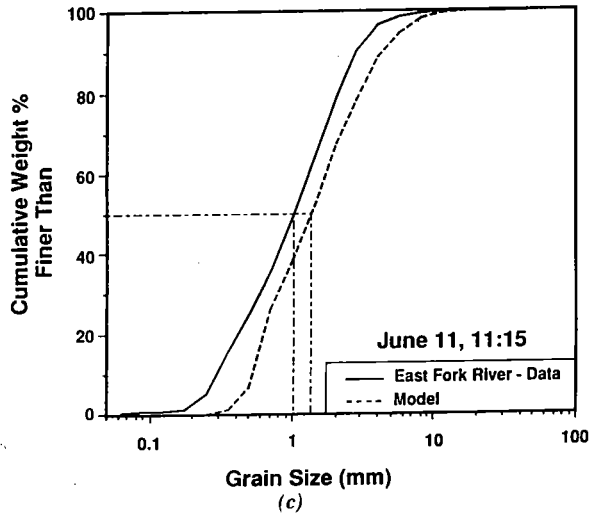

(c)

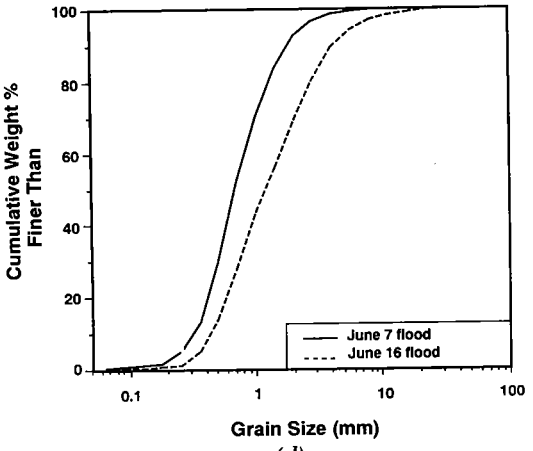

(d)

FIG. 8. (c) At 11:15 on June 11; and (*d*) Comparison of June 7 and June 16 Flood Events for East Fork River

application of MIDAS, the computation time of this study provides an indication of computer requirements. This study used 20 grain sizes of a single mineral density (quartz) as bed material, at 16 locations along the stream, and ran a total of 6,912 timesteps (12 time steps/hr · 24 hr/day · 24 days). The MIDAS FORTRAN code ran just over 12 hr on an HP 300 series workstation using a floating point accelerator.

Gold Placer Study

MIDAS has been developed specifically to treat multiple grain densities, and therefore to provide insight into the genesis of heavy mineral placers.

To demonstrate the use of MIDAS in this regard, an experiment was performed to simulate gold accumulation in an aggrading alluvial fan. Such a setting has been postulated for the origin of some of the Witwatersrand paleoplacers of South Africa, the richest gold deposits in the world (Pretorius 1976). The experiment roughly approximates the paleohydraulic conditions, which are thought to have formed the 2.8 Ga Ventersdorp Contact Reef, a paleoplacer of the Witwatersrand Basin. The modeled slope and total weight percentage of gold are not reasonable estimates, because we attempted to model an aggradational system where temporal and longitudinal gold grade variations could be observed. The model consists of a 5-km long river of constant width equal to 100 m and constant discharge equal to 100 m^3s^{-1} flowing over a flat surface with a slope of 0.0001 into a standing body of water with a surface elevation equal to 4.75 m above the bed. A temporally constant, ϕ normally distributed, sediment feed of quartz, gold, and pyrite is allowed to enter at the river head. The grain size distributions are summarized in Table 3. The sediment feed rates of the grain sizes, expressed in kg $m^{-1}s^{-1}$, are equal to the weight proportion of the grains at the start of the run. For example, if a grain size makes up 1% of the bed, its feed rate is 0.01 kg $m^{-1}s^{-1}$. Pyrite, while not a major bed constituent in modern rivers, is a major constituent of the Witwatersrand gold paleoplacers, which were deposited before the earth had an oxygen-rich atmosphere (Pretorius 1976).

Results (Fig. 9) show that the initial stream power of the river cannot transport the mixture at the feed rate, causing sediment to accumulate at upstream nodes. Gradually, as more material is deposited, the bed slope increases, and a concave profile alluviates and expands. The gold and pyrite are preferentially deposited at certain downstream locations, where conditions are favorable for placer genesis (Figs. 10 and 11). The ideal placer locations are a function of many factors, the main two being heavy mineral grain size and bed shear stress, the latter in turn a function of bed slope and downstream distance. After 1.75 yr (Fig. 10), the first 1,200 m of the stream show, on average, a bed enriched in relatively coarse gold, whose concentration steadily decreases with distance, while the following 1,500

TABLE 3. Grain Size Distributions Used in Gold Placer Simulation

Quartz		Pyrite		Gold	
Grain size interval (mm) (1)	Weight (%) (2)	Grain size interval (mm) (3)	Weight (%) (4)	Grain size interval (mm) (5)	Weight (%) (6)
0.125–0.250	0.437	0.008–0.016	0.044	0.008–0.011	0.005
0.250–0.500	1.489	0.016–0.031	0.149	0.011–0.016	0.017
0.500–1.000	3.965	0.031–0.062	0.397	0.016–0.022	0.044
1.000–2.000	8.266	0.062–0.125	0.827	0.022–0.031	0.092
2.000–4.000	13.489	0.125–0.250	1.349	0.031–0.044	0.150
4.000–8.000	17.232	0.250–0.500	1.723	0.044–0.062	0.191
8.000–16.00	17.232	0.500–1.000	1.723	0.062–0.088	0.191
16.00–32.00	13.489	1.000–2.000	1.349	0.088–0.125	0.150
32.00–64.00	8.266	2.000–4.000	0.827	0.125–0.177	0.092
64.00–128.0	3.965	4.000–8.000	0.397	0.177–0.250	0.044
128.0–256.0	1.489	8.000–16.00	0.149	0.250–0.354	0.017
256.0–512.0	0.437	16.00–32.00	0.044	0.354–0.500	0.005

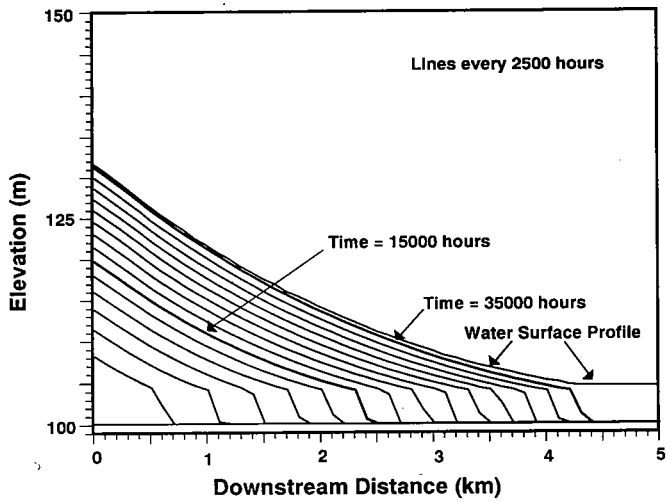

FIG. 9. Computed Temporal Evolution of Alluvial Fan

meters are depleted. Beyond 2,700 meters downstream, the river bed returns to its original concentration because the bed has not yet been altered due to deposition or erosion. Relatively fine-grained gold, also with an original weight percentage of 0.158% in the bed and feed, is depleted over the first 500 m. Over the next 2,200 m, its weight percentage steadily increases on average to eventually peak at 2,500 m downstream. The intermediate size gold, with an original weight percentage of 0.682 in the bed and feed, shows a bell-shaped concentration curve, with a peak at 1,500 m downstream. The origins of these distributions may be explained as follows. The relatively coarse-sized gold, due to its size and high specific gravity, is entrained only at high shear stresses. Once it enters the river system, it is not transported very far, thus accounting for its enrichment at the stream head. Between 1,200 and 2,700 m downstream, the concentration is low because the original bed, where relatively coarser gold made up 0.158%, has by now been buried by sediment impoverished in coarse gold. Relatively fine gold on the other hand, is readily entrained under the stream shear stresses, and as a result is found over the length of the river. The fact that its bed weight percentage is greater than that of the feed seems to indicate that on the whole the gold is more difficult to transport than quartz. Its preferential deposition at 2,500 m seems to indicate that fine-grained gold is transported reasonably well by the river system and is deposited when the flat slope is reached at 2,700 m. The intermediate-sized gold shows an intermediate behavior. At the head of the stream, the flow can entrain it and transport it downstream. At about 1,500 m downstream, the bed shear stress has dropped below a value at which, on average, the medium-grained gold is entrained and transported, resulting in gold deposition. While still partially entrainable after 1,500 m, most of the medium-grained gold will not be entrained or transported past this point. The longitudinal downstream variation of the pyrite weight percentages (Fig. 11) is analogous to that of gold. They show bell-shaped distributions, with the optimal zone of concentration a function of grain size.

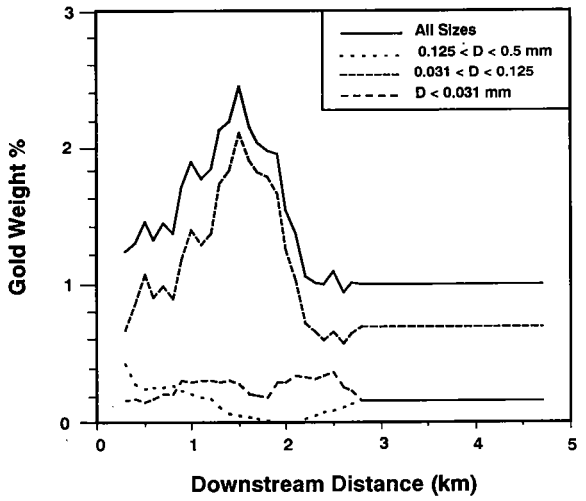

FIG. 10. Moving Average (n = 5) of Gold Weight Percentage in Bed as Function of Grain Diameter and Downstream Distance at 15,000 hrs for Gold Placer Study

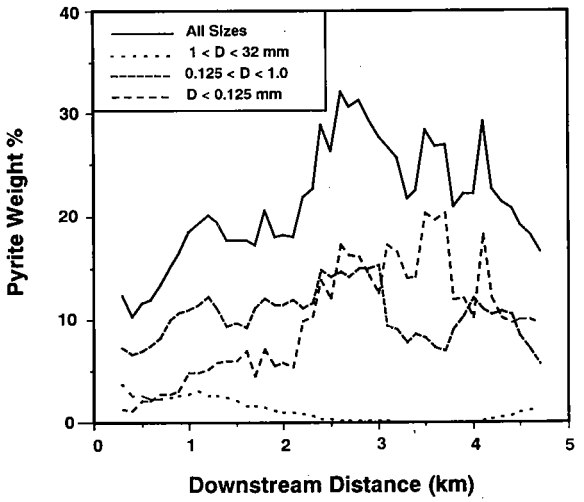

FIG. 11. Moving Average (n = 5) of Pyrite Weight Percentage in Bed as Function of Grain Diameter and Downstream Distance at 35,000 hr for Gold Placer Study

CONCLUSIONS

A one-dimensional numerical model of heterogeneous size-density sediment transport has been used to reproduce the movement of graded sediments in a number of natural and laboratory flow reaches. Accurate predictions of bed and armor-layer grain size distributions, eroded grain size distributions, eroded thicknesses, and total bedload transport rates were

obtained when the model was tested against a flume study of Little and Mayer, two flume studies of Ashida and Michiue, the canal study of Lane and Carlson, and a one-month period of the East Fork River data set collected by the U.S. Geological Survey. The model was also used to simulate the behavior of dense minerals in an alluvial fan setting, providing credible estimates of their zone of maximum enrichment along a longitudinal river profile. The main advantage of this model over others is the high degree of accuracy of model results obtained using only bed and flow variables as input.

Acknowledgments

The writers would like to express their grateful appreciation to the South Africa Chamber of Mines Research Organization for their financial support of this project. They would also like to thank Dr. C. James and Dr. P. Fleming for their input and output during the model development, and anonymous reviewers for their helpful criticism of an earlier version of the article.

Appendix I. References

Ashida, K., and Michiue, M. (1971). "An investigation of river bed degradation downstream of a dam." *Proc., 14th Congress of the Int. Assoc. for Hydraulic Research,* 3, 247–256.

Borah, D. K., Alonso, C. V., and Prasad, S. N. (1982). "Routing graded sediments in streams: Applications." *J. Hydr. Div.,* ASCE, 108(12), 1504–1517.

De Vries, M. (1973). "River-bed variations—Aggradation and degradation." *Publications No. 107, Delft Hydraulics Laboratory,* Delft, The Netherlands.

Lane, E. W., and Carlson, E. J. (1953). "Some factors affecting the stability of canals constructed in coarse granular material." *Proc. Int. for Hydraulic Research,* ASCE, New York, N.Y., 37–48.

Leopold, L. B., and Emmett, W. W. (1976). "Bedload measurements, East Fork River, Wyoming." *Proc., Nat. Acad. of Sci.,* 73(4), 1000–1004.

Little, W. C., and Mayer, P. G. (1972). "The role of sediment gradation on channel armoring." *Publication No. ERC-0672,* School of Civil Engineering in Cooperation with Environmental Research Center, Georgia Institute of Technology, Atlanta, Ga. 1–104.

Mahoney, H. A., Andrews, E. D., Emmett, W. W., Leopold, L. B., Meade, R. H., Myrick, R. M., and Nordin, C. F. (1976). "Data for calibrating unsteady-flow sediment transport models, East Fork River, Wyoming, 1975." *Open File Report 76-22,* U.S. Geological Survey, Denver, Colo. 1–293.

Pretorius, D. A. (1976). "The nature of the Witwatersrand gold-uranium deposits." *Handbook of strata-bound and stratiform ore deposits.* K. H. Wolf, ed., Elsevier Scientific Publishing Co., New York, N.Y., 29–52.

van Niekerk, A., Vogel, K. R., Slingerland, R. L., and Bridge, J. S. (1992). "Routing of heterogeneous sediments over movable bed: Model development." *J. Hydr. Engrg.,* ASCE, 116(2), pages, this issue.

Appendix II. Notation

The following symbols are used in this article:

a = height of moving bed layer (m);
D_{ij} = grain diameter of grain size fraction i of mineral density j (m);
D_{50} = median grain diameter of active layer (m);
T_a = active layer thickness (m);

Θ_c = dimensionless critical Shields parameter, equal to critical shear stress necessary to entrain a grain, divided by submerged weight of grain;
Θ_{cij} = dimensionless critical shear stress necessary to entrain size-density fraction ij;
Θ_{c50} = dimensionless critical shear stress necessary to entrain median grain diameter;
$\bar{\tau}'$ = time-averaged, effective median bed shear stress (Pa); and
τ_{c50} = critical shear stress necessary to entrain median grain size (Pa).

Subscripts

i = grain size interval;
j = mineral density; and
50 = of 50th percentile of bed grain size distribution.